

2

**DTIC  
SELECTE  
S D**

1a. SECURITY CLASSIFICATION Unclassified		1b. RESTRICTIVE MARKINGS None
2a. SECURITY CLASSIFICATION AUTHORITY		3. DISTRIBUTION / AVAILABILITY OF REPORT Unrestricted
b. DECLASSIFICATION / DOWNGRADING SCHEDULE 1992		5. MONITORING ORGANIZATION REPORT NUMBER(S)
4. PERFORMING ORGANIZATION REPORT NUMBER(S)		

5a. NAME OF PERFORMING ORGANIZATION Rensselaer Polytechnic Institute	6b. OFFICE SYMBOL (if applicable)	7a. NAME OF MONITORING ORGANIZATION
5c. ADDRESS (City, State, and ZIP Code) Materials Engineering Department Troy, NY 12180-3590		7b. ADDRESS (City, State, and ZIP Code) <b>DISTRIBUTION STATEMENT A</b> Approved for public release; Distribution Unlimited

8a. NAME OF FUNDING / SPONSORING ORGANIZATION Office of Naval Research	8b. OFFICE SYMBOL (if applicable) Code 1131M	9. PROCUREMENT INSTRUMENT IDENTIFICATION NUMBER	
8c. ADDRESS (City, State, and ZIP Code) 800 North Quincy Street Arlington, VA 22217		10. SOURCE OF FUNDING NUMBERS	
PROGRAM ELEMENT NO.	PROJECT NO. N00014 90-J 1439	TASK NO.	WORK UNIT ACCESSION NO.

11. TITLE (Include Security Classification)  
The Effect of Flow Rates on the Localized Corrosion Behavior of 304 Stainless Steel in Ozonated 0.5N NaCl

12. PERSONAL AUTHOR(S)  
B. E. Brown, H. H. Lu and D. J. Duquette

13a. TYPE OF REPORT Technical	13b. TIME COVERED FROM _____ TO _____	14. DATE OF REPORT (Year, Month, Day) 1991 December 15	15. PAGE COUNT 22
----------------------------------	--	---	----------------------

16. SUPPLEMENTARY NOTATION

17. COSATI CODES			18. SUBJECT TERMS (Continue on reverse if necessary and identify by block number) Localized Corrosion, Ozone, Passivation, Repassivation
FIELD	GROUP	SUB-GROUP	

19. ABSTRACT (Continue on reverse if necessary and identify by block number)  
The effect of flow on 304 stainless steel in a solution of 0.5N NaCl containing O<sub>2</sub>, 0.02, and 1.2 mg/liter dissolved ozone was studied at room temperature. Flow rates ranging from 0.3 to 2.0 m/s were simulated by the use of a Rotating Cylinder Electrode (RCE). Corrosion potentials and net current densities were measured and values of breakdown and repassivation potentials were derived from cyclic polarization curves. It was found that the transition from laminar to turbulent flow for this system occurs between 0.25 and 0.35 m/s, based on the inverse relationship observed between the breakdown and repassivation potential, as well as the changes in the net current density. Under laminar flow conditions, increasing velocity shifted the repassivation potential in the active direction due to an increase in the driving force for pitting which resulted from the stabilization of the passive film, this stabilization was also reflected by an increase in the breakdown potential in the

20. DISTRIBUTION / AVAILABILITY OF ABSTRACT <input checked="" type="checkbox"/> UNCLASSIFIED/UNLIMITED <input type="checkbox"/> SAME AS RPT. <input type="checkbox"/> DTIC USERS		21. ABSTRACT SECURITY CLASSIFICATION	
22a. NAME OF RESPONSIBLE INDIVIDUAL D. J. Duquette		22b. TELEPHONE (Include Area Code) (518) 276-6459	22c. OFFICE SYMBOL

19. Abstract (Continued)

noble direction. Values of the net current density decreased with increasing velocity in this regime, due to a decrease in the diffusion boundary layer at the alloy surface. High ozone concentrations further decreased the magnitude of the net current density due to the limiting current density of ozone increasing with concentration. Under turbulent flow conditions, increased velocity caused the net current density to stabilize in deaerated and low ozone concentration solutions, however, solutions containing high concentrations of ozone experienced an increase in net current density to values similar to stagnant solutions, indicating that turbulence actually reduces the concentration gradient of ozone at the surface. Similarly, values of the breakdown and repassivation potentials revert to those of stagnant conditions in the turbulent region. The corrosion potentials of deaerated solutions increased with increasing flow rates due to the cathodic reaction of hydrogen evolution being controlled by diffusion at the surface of the sample, while increasing velocity had no effect on the corrosion potential of ozonated solutions due to the noble redox potential of ozone.

**The Effect of Flow Rates on the Localized Corrosion Behavior  
of 304 Stainless Steel in Ozonated 0.5N NaCl**

B.E. Brown, H.H. Lu and D.J. Duquette  
Materials Engineering Department  
Rensselaer Polytechnic Institute  
Troy, New York 12180-3590

**92-01180**



**Technical Report  
December 1991**

**Office of Naval Research  
N-00014-90-J-1439**

This report is unclassified. Reproductions and distribution for any purpose of the U.S. government is permitted.

**92 1 13 088**

**Abstract**

The effect of flow on 304 stainless steel in a solution of 0.5N NaCl containing 0, 0.02, and 1.2 mg/liter dissolved ozone was studied at room temperature. Flow rates ranging from 0.3 to 2.0 m/s were simulated by the use of a Rotating Cylinder Electrode (RCE). Corrosion potentials and net current densities were measured and values of breakdown and repassivation potentials were derived from cyclic polarization curves. It was found that the transition from laminar to turbulent flow for this system occurs between 0.25 and 0.35 m/s, based on the inverse relationship observed between the breakdown and repassivation potential, as well as the changes in the net current density. Under laminar flow conditions, increasing velocity shifted the repassivation potential in the active direction due to an increase in the driving force for pitting which resulted from the stabilization of the passive film, this stabilization was also reflected by an increase in the breakdown potential in the noble direction. Values of the net current density decreased with increasing velocity in this regime, due to a decrease in the diffusion boundary layer at the alloy surface. High ozone concentrations further decreased the magnitude of the net current density due to the limiting current density of ozone increasing with concentration. Under turbulent flow conditions, increased velocity caused the net current density to stabilize in deaerated and low ozone concentration solutions, however, solutions containing high concentrations of ozone experienced an increase in net current density to values similar to stagnant solutions, indicating that turbulence actually reduces the concentration gradient of ozone at the surface. Similarly, values of the breakdown and repassivation potentials revert to those of stagnant conditions in the turbulent region. The corrosion potentials of deaerated solutions increased with increasing flow rates due to the cathodic reaction of hydrogen evolution being controlled by diffusion at the surface of the sample, while increasing velocity had no effect on the corrosion potential of ozonated solutions due to the noble redox potential of ozone.

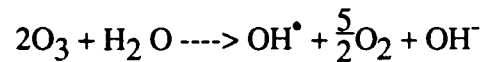
for
<input checked="" type="checkbox"/>
<input type="checkbox"/>
<input type="checkbox"/>

Availability Codes	
Dist	Avail and/or Special
<i>A-1</i>	



## **Introduction**

Molecular ozone is a strong oxidizer, having a standard electrode potential of 2.07V (vs SHE).<sup>1</sup> The decomposition of ozone in water can be represented by the following reaction:



Dissolved ozone has been shown to cause the corrosion potential and the breakdown potential of 304L stainless steel to shift to more noble values for ozone concentrations of less than 0.2 mg/liter in 0.5N NaCl.<sup>2</sup> These noble shifts suggest that the cathodic reduction of ozone controls the mixed potential, and that ozone provides a driving force for further stabilization of the passivating film on stainless steel.

Ozone is being increasingly recommended for use in cooling water systems in order to reduce corrosion, scaling, and biofouling. These systems can experience flow rates from 0-3 m/s. This study reports an investigation of the effects of flow in combination with dissolved ozone.

There are at least two possible methods available to study the effect of flow rate on an electrode. One method involves moving the electrolyte past a fixed electrode to create flow. The other method involves rotating the electrode in the electrolyte. The latter technique was chosen, and a Rotating Cylinder Electrode (RCE) was implemented in this investigation.

When considering flow over a surface, the value of the critical Reynold's number is of interest. This number can be used to calculate the velocity at which the transition from laminar to turbulent flow occurs. This transition is important because it helps explain the rate controlling factors of the corrosion reaction at the metal surface. Turbulent flow causes a mixing of adjacent fluid layers, therefore transport of reactants and products to and away from the surface of a sample will not be the rate limiting factor for the corrosion reaction,

laminar flow, on the other hand, causes the reaction to become diffusion limited due to the stagnant fluid layer near the surface.<sup>3</sup>

If the critical Reynold's number is known for a system, the critical velocity (m/s) above which the transition from laminar to turbulent flow occurs can be calculated using the formula:

$$V = \frac{(vR_e)}{R} \quad (1)$$

where  $v$  is the kinematic viscosity of the fluid in units of  $\text{m}^2 \text{s}^{-1}$  and  $R$  is the radius of the cylinder in meters.<sup>4</sup> While very little scientific literature exists characterizing the fluid behavior of the RCE with reference to the critical Reynold's number, Mallock has stated that the critical Reynold's number for laminar to turbulent flow for this system is 1900.<sup>5</sup> Using this value of the Reynold's number in Equation (1), and approximating the kinematic viscosity of 0.5N NaCl at 25°C as being  $1.1 \times 10^{-6} \text{ m}^2/\text{s}$ , the transition velocity for laminar to turbulent flow was calculated to be 0.22 m/s for our system.<sup>6</sup> This indicates that for experiments in which the velocity is above 0.22 m/s, flow will be in the turbulent region.

In the case studied here, it is expected that increasing the flow rate will lead to increased rates of oxygen and/or ozone transfer from the bulk electrolyte to the electrode surface. If oxygen or ozone reduction controls the mixed potential, then increased amounts of these reactants at the surface of the electrode should increase the mixed, or corrosion potential. It has been reported that increasing the flow rate from 0.05 to 1.7 m/s in natural water containing ozone has no effect on the corrosion rates of 304 stainless steel.<sup>7</sup> Passive current density values taken from potentiodynamic scans, however, were observed to decrease with the onset of rotation for 304 stainless steel in 3.5% NaCl.<sup>8</sup>

### **Experimental Procedure**

304 stainless steel bar stock was cut into cylinders 1.27 cm in length and 1.905 cm in diameter. The composition of the alloy is shown in Table I. A hole was drilled down

the center of each cylinder for fixturing. The samples were wet ground to 600 grit SiC and rinsed with distilled water prior to testing.

Figure 1 shows a schematic diagram of the experimental apparatus used in this study. A stainless steel rod was used as a fixture for the cylindrical metal samples, as shown in Figure 2. The rod was insulated from the electrolyte by means of Teflon sheaths and Buta-N O-rings. A dimpled glass bead was fused to the bottom of the electrochemical cell in order to stabilize the fixture while operating.

A conventional motor was used to rotate the electrode. A tachometer was used to determine the rotation speed in RPM of the electrode at different motor settings. The velocity (m/s) of the electrode was calculated using the formula:

$$V = \frac{\pi f R}{30} \quad (2)$$

where  $f$  represents the rotation speed in RPM, and  $R$  is the radius of the electrode in meters.<sup>7</sup> Flow rates between 0 and 2 m/s were examined using this apparatus.

Electrical connection was maintained between the rod and the cylindrical metal sample by a stainless steel wire, spot welded onto both pieces. A copper brush, in contact with the rotating stainless steel rod, was used to electrically connect the sample and the potentiostat during rotation.

The aqueous solution utilized was 0.5N NaCl acidified to a pH of 5 with HCl at room temperature ( $25^{\circ}\pm 3^{\circ}\text{C}$ ). Test solutions containing no ozone were deaerated by bubbling argon gas through the solution for two or more hours. Ozonated solutions were produced using a commercial corona discharge ozone generator. Ozone was bubbled into the solutions for at least twelve hours prior to, as well as during, experimentation. Ozone concentrations were measured prior to each experiment, in a stagnant solution, using the standard DPD method.<sup>9</sup>

Experiments were performed for conditions of 0, 0.02, and 1.2 mg/liter of dissolved ozone, with flow rates varying from 0 to 2.0 m/s. Samples were conditioned at a

potential of -1.0 V versus SCE for five minutes before measuring the free corrosion potential,  $E_{\text{CORR}}$ , as a function of time. Values of corrosion potential were obtained, after being allowed to stabilize for 4000 seconds. For voltametry experiments, the potential was stepped to -600 mV vs. SCE and subsequently polarized in the anodic direction to +500 mV vs. SCE, followed by polarization in the cathodic direction. Typical polarization curves are shown in Figure 3.<sup>2</sup> The pitting, or breakdown potential,  $E_b$ , and the repassivation potential,  $E_p$ , were measured using conventional criterion.<sup>10,11</sup> Three experiments were performed for each condition, and the results were averaged.

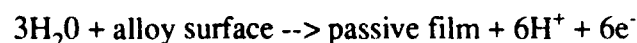
Net current density data was obtained after conditioning the samples at -1000 mV for five minutes and then setting the potential to a constant value of -100 mV. Readings were taken after ten minutes at the constant potential.

## **Results and Discussion**

The results of flow rates and dissolved ozone concentrations on corrosion potentials, breakdown potentials, and the repassivation potentials are summarized in Table II and shown in Figures 4-6.

### **Corrosion Potential**

Figure 4 shows the steady state corrosion potential measurements for the 304 stainless steel as a function of solution flow rate and dissolved ozone concentration. In a deaerated solution the corrosion potential monotonically shifts in the noble direction with increasing solution velocity, with only a small amount of scatter for each data set. These results suggest that, even for the nominally low passive current densities observed in deaerated, near neutral solutions, the cathodic reaction which supports anodic polarization is diffusion controlled. Uhlig has suggested that only water is required to induce passivity in stainless steels according to the anodic reaction:<sup>12</sup>



The cathodic reaction in a deaerated solution can be assumed to be the hydrogen reaction:





Since the hydrogen ion is provided by the anodic reaction, diffusion of the ion to the surface for reduction is not required. Accordingly, it appears that either surface diffusion of H to form  $\text{H}_2$ , or the stifling of active surface sites for the reduction of the  $\text{H}^+$  ion, control the cathodic reaction rate, effectively shifting the corrosion potential in the noble direction.

When ozone is admitted to the solution, in any concentration greater than 0.02 mg/l, the noble shift in potential, due to the noble redox potential of the ozone, fixes the corrosion potential and the solution velocity no longer becomes a controlling factor. In any event, with ozone present in the solution the corrosion potential is well within the passive current density regime and ozone does not affect the free corrosion behavior of the alloy.

### **Breakdown and Repassivation Potentials**

Figure 5 shows the variation of the breakdown, or pitting potential, with solution velocity. For the deaerated solutions, the breakdown potential is shifted in the noble direction as velocity is increased, reaching a maximum at a flow rate of 0.3 m/s. At higher solution velocities the breakdown potential reverts to essentially the same value as is observed in stagnant solutions.

Similar behavior is observed for solutions which contain 0.02 mg/l ozone, except that the noble shift in the breakdown potential occurs between 0.3 and 0.5 m/s. At ozone levels of 1.2 mg/l, solution flow rates do not appreciably affect breakdown potentials, although a slight noble shift in the breakdown potential is observed at solution velocities between stagnant and 0.5 m/s. An examination of the repassivation potentials, shown in Figure 6, indicates an inverse relationship with velocity when compared with the breakdown potentials for deaerated solutions, as well as for solutions containing 0.02 mg/l ozone. That is, there is a minimum in repassivation potential at velocities of 0.3-0.5 m/s, however, the potentials revert to essentially the same values when solution velocities are increased beyond this. At ozone concentrations of 1.2 mg/l, there is a slight shift in the

noble direction of the repassivation potential as active flow is induced, but velocity has no further effect on the repassivation potential.

As has been indicated, turbulent flow occurs when the velocity of the fluid exceeds a critical velocity. The results obtained in this study indicate a transition velocity of approximately 0.25 - 0.35 m/s, based on the changes which were observed in the repassivation and breakdown potential in this region. This is in good agreement with the theoretical calculation of a critical velocity of 0.22 m/s, which was based on a critical Reynold's number of 1900. Below the critical velocity, laminar flow dominates. Thus, under laminar flow conditions, increasing flow rates stabilize passivity against pit initiation by chlorides, while under turbulent flow conditions, water velocity has little or no effect on pit initiation in deaerated chloride solutions, or in solutions containing only small amounts of ozone. This behavior is believed to be due to the availability of the passivating species to the alloy surface. In order for pitting to occur, chloride must adsorb on the passive film. Increasing solution velocities allow other ionized species to preferentially adsorb on the passive film, thus blocking localized film breakdown by increasing surface coverage. When ozone is present in the solution, increasing velocities provide increasing amounts of ozone to react on the surface thus stabilizing passivity. If sufficient ozone is present in the solution, sufficient reduction of the ozone occurs such that increasing solution velocities do not appreciably affect the breakdown potential.

With reference to the repassivation potential, increasing solution velocity in the laminar regime shifts the potential in the active direction. Further increases in velocity, which result in turbulent flow, cause the repassivation potential to revert to that which is observed in stagnant solutions. This behavior is apparently associated with the larger driving force for active/passive cell corrosion which is caused by increasing the stability of the passive film due to competitive adsorption of passivators vs. chloride. According to this hypothesis, the potential difference between the passive surface and the pit interiors is maximized by this process and, accordingly, pits remain active to less noble applied

potentials. When turbulent flow occurs, the relative delivery of passivating species and chloride reverts to similar conditions as for stagnant solutions. With small amounts of ozone as a passivator, the repassivation potential responds in a similar manner to non-ozonated solutions except that increasing the velocity into the turbulent region of flow does not shift the repassivation potential to as noble a value as is observed for non-ozonated solutions. For larger amounts of ozone in solution the presence of ozone results in a virtually constant repassivation potential as a function of velocity, presumably because sufficient ozone is always present to retain the alloy surface in the same passive state.

### **Passive Current Density**

The net current densities for the stainless steel, measured at -100 mV vs. SCE are shown in Figure 7. This data indicates that increasing flow rates decrease the net currents until flow rates of 0.3-0.5 m/s are achieved, in agreement with the results obtained for the corrosion potential, the breakdown potential, and the repassivation potential. Further, the magnitude of the net current density decreases with increasing concentrations of dissolved ozone. For the case of deaeration, or for a dissolved ozone concentration of 0.02 mg/l, the value of the net current density becomes essentially constant with the onset of turbulent flow. At a relatively high ozone concentration of 1.2 mg/l, the net current density increases after the onset of turbulent flow, reaching essentially the same value as that observed in a stagnant solution.

These results show that the cathodic reduction of either  $H^+$  (in the deaerated solution) or  $O_3$  (in ozonated solutions) is controlled by concentration polarization. In a stagnant deaerated solution of pH 5, the limiting current density for the reduction of  $H^+$  is of the order of  $-2 \times 10^{-6} \text{ A/cm}^2$ . Since the diffusion boundary layer decreases with increasing flow rates (convection), the absolute value of the limiting current density will increase and the net current density measured at the alloy surface will decrease. However, with the onset of turbulent flow, convection in the boundary layer is destabilized and the net current reaches a constant value. The addition of ozone to the solution results in an

additional reduced specie which can be expected to shift the net current density in the cathodic direction. However, at the lower concentrations of ozone examined in this study (0.02 mg/l), the additive limiting current density is only of the order of  $\sim -10^{-7}$  A/cm<sup>2</sup> and accordingly has little effect on the measured net current density. Increasing the flow rate results in a measurable increase in the limiting current density for the reduction of the ozone (which is reduced with the acceptance of six electrons in contrast to one electron for the H<sup>+</sup>). The net current density is accordingly decreased, and reaches a constant value when turbulent flow occurs. At the highest level of ozone examined in this study (1.2 mg/l), the limiting current density for ozone reduction is approximately  $-3 \times 10^{-6}$  A/cm<sup>2</sup>, and a significant shift in the net current density in the cathodic direction is observed, even in stagnant solutions. With increasing rates of laminar flow, the cathodic reduction limiting current density and the resultant net current, become still more negative. In contrast to either deaerated solutions, and solutions containing small amounts of ozone, the onset of turbulent flow apparently causes a reversal in the trend for the net current density. This reversal is believed to be due to turbulence carrying unreduced dissolved ozone away from the alloy surface, as well as to the surface. This behavior effectively reduces the ozone concentration gradient and accordingly reduces the magnitude of the limiting current density associated with ozone reduction. In any event, all of the changes in the electrochemical parameters associated with dissolved ozone can be ascribed to the kinetics associated with the ozone reduction. There is no evidence that the inherent passivity of the alloy surface is affected by the presence of ozone. In fact, in a previous study it was shown, by Auger electron spectroscopy, that the thickness and composition of the passive films on stainless steels are unchanged by dissolved ozone in aqueous solutions.<sup>2</sup>

## **Conclusions**

1. The critical velocity at which the transition from laminar to turbulent flow occurs was found to be between 0.25 and 0.35 m/s for this system, based on maxima and minima that were observed in the breakdown and repassivating potentials. This result is in good agreement with a theoretical critical Reynold's number for the transition from laminar to turbulent flow of 1900.
2. In the case of laminar flow conditions, below 0.25 m/s, increasing flow rates increased the breakdown potential, indicating increased stability of the passive layer against pit initiation due to the blocking of chloride ion adsorption by other ionized species adsorbing on the passive film. This increase in stability of the passive film caused the repassivation potential to become more active due to the increased potential difference between the passive surface and the existing pits.
3. In the case of turbulent flow conditions, increasing the flow rate in this region caused the breakdown and repassivation potentials to revert values of stagnant solutions, therefore indicating that the relative delivery of passivators and chloride ions is similar to that of a stagnant solution.
4. Increased ozone concentrations further stabilized passivity, however, increasing velocity had little effect on solutions of high enough ozone concentration.
5. With increasing flow rates, the corrosion potential, in the case of deaerated solutions, increased due to the cathodic reaction of hydrogen evolution at the surface being diffusion controlled. In the case of ozonated solutions, velocity had no effect on the corrosion potential due to the noble redox potential of the ozone.

6. Increasing flow rates in the laminar regime caused the net current density to decrease due to an increase in the limiting current density caused by shrinkage of the diffusion boundary layer. Increasing ozone concentration showed a larger reduction in net current density for this regime due to the direct relationship between concentration and the limiting current density. Transition into the turbulent region caused the diffusion layer to break down, stabilizing values of the net current density for deaerated solutions and solutions with small amounts of dissolved ozone. For higher concentrations of dissolved ozone, the values of the limiting current density stabilized to those of stagnant conditions, indicating a decrease in the concentration gradient of ozone at the alloy surface.

### **Acknowledgment**

The authors would like to acknowledge the support of the U.S. Office of Naval Research under grant N-00014-90-J-1439.

## **References**

1. A.J. Bard, L.R. Faulkner, Electrochemical Methods: Fundamentals and Applications (New York, NY: John Wiley and Sons, 1980), p. 700.
2. H.H. Lu, D.J. Duquette, *Corrosion* 46(1991): p. 843.
3. R.W. Fox, H.J McDonald, Introduction to Fluid Mechanics (New York, NY: John Wiley and Sons, 1980).
4. M. Eisenberg, C.W. Tobias, and C.R. Wilke, *J. Electrochem. Soc.*, 101 (1954): p. 306.
5. A. Mallock, *Phil. Roy. Soc.*, A187 (1896): p. 41.
6. J. A. Roberson, C. T. Crowe, Engineering Fluid Mechanics (Boston, MA: Houghton Mifflin Company, 1980) pp. 643-644.
7. M. Matsudaira, M. Suzuki, and Y. Sato, *Matsl. Perform.* 21(1981): p. 55.
8. F. Mansfeld, J.V. Kenkel *Corrosion* 35(1979): p. 43.
9. J.W. Oldfield, B. Todd, *Desalination* 38 (1981): p. 233.
10. M. Hubbfell, C. Price, and R. Heidersbach, in Laboratory Corrosion Tests and Standards (Philadelphia, PA: ASTM, 1985), p. 324.
11. J. Tousek, Theoretical Aspects of Localized Corrosion of Metals (Switzerland: Trans Tech Publications LTD, 1985).
12. H.H. Uhlig, R.W. Revie, Corrosion and Corrosion Control (New York, NY: John Wiley & Sons, 1985), p. 71.

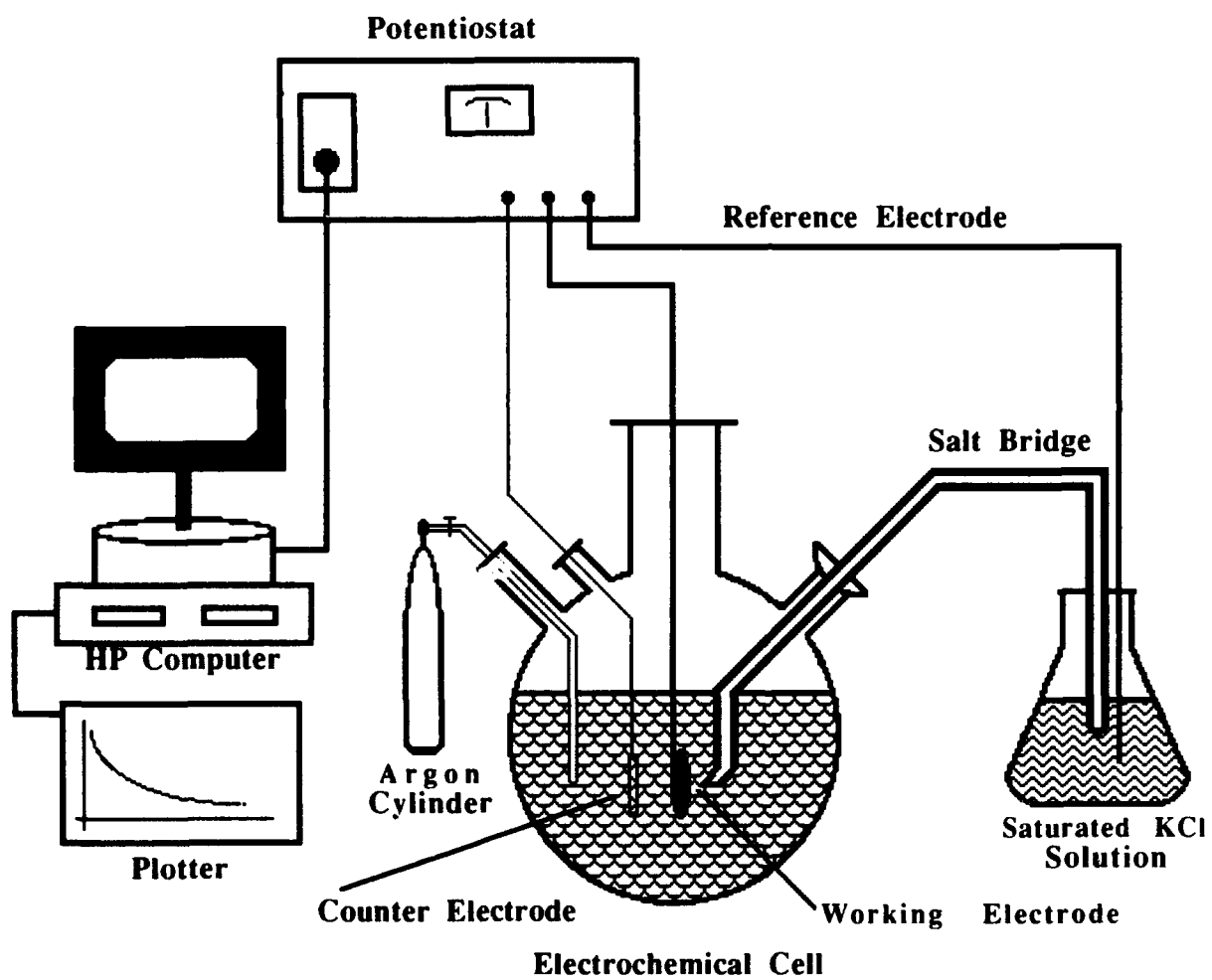


**Figure 1. Schematic diagram of corrosion study apparatus**



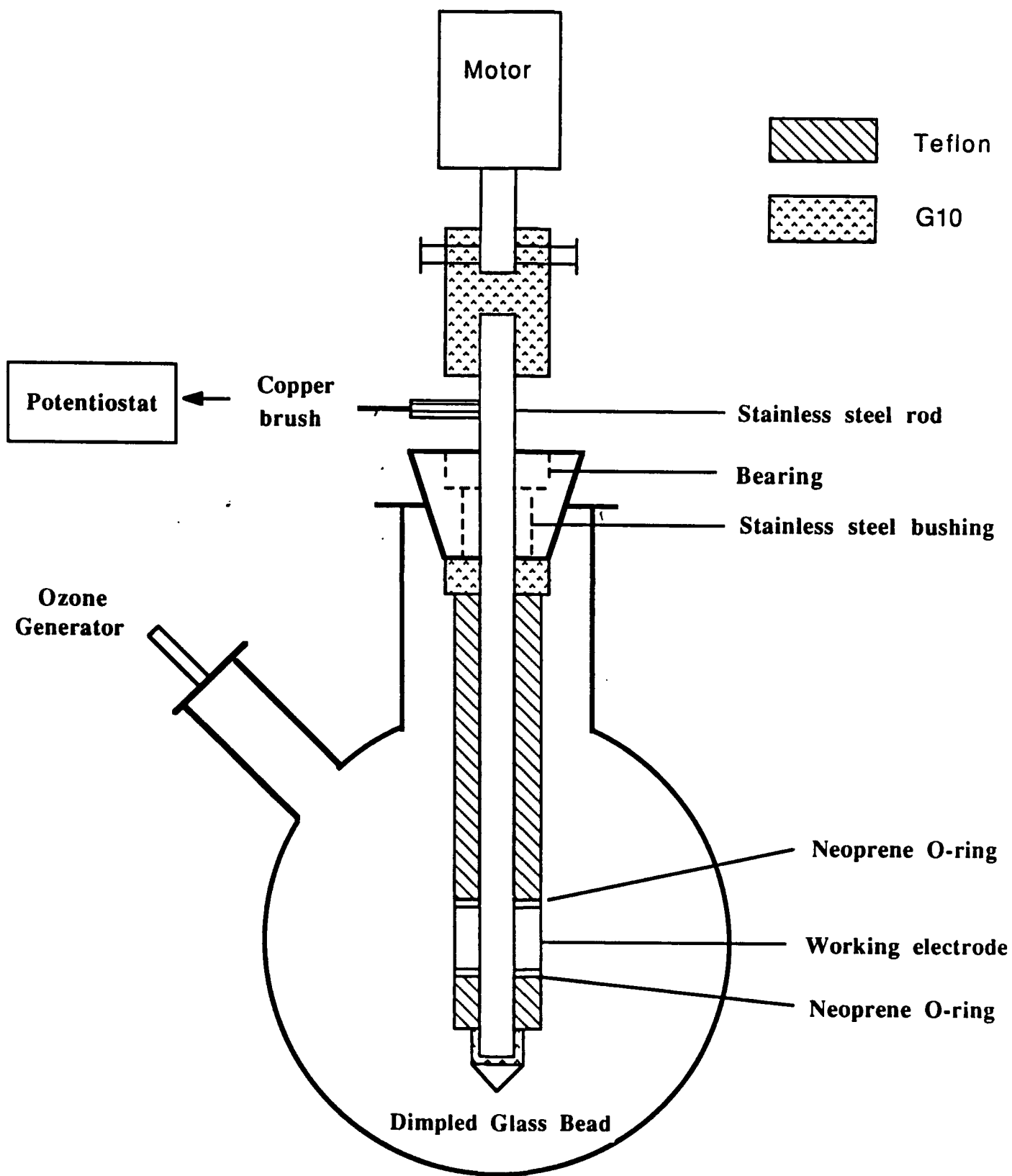


**Figure 2. Detail of the experimental set-up**

**Table I. Chemical composition of 304 Stainless steel used in this study (wt%)**

<b>C</b> max.	<b>Mn</b> max.	<b>P</b> max.	<b>S</b> max.	<b>Si</b> max.	<b>Cr</b>	<b>Ni</b> max.	<b>Cu</b> max.	<b>Mo</b> max.
0.08	2.0	0.04	0.030	1.0	18-20	10.3	0.75	0.75

**Table II. Average values of corrosion potential, breakdown potential and repassivation potential of 304 SS for variable ozone concentrations and rotation speeds in 0.5N NaCl solution**

C(O <sub>3</sub> ) (mg/l)	Flow rate (m/s)	E <sub>corr</sub> (mV)	E <sub>b</sub> (mV)	E <sub>p</sub> (mV)
0	0	-464	200	-23
	0.33	-411	268	-83
	0.58	-386	186	-125
	0.86	-384	182	-10
	2.03	-302	213	-29.3
0.02	0	-111	274	-65
	0.33	21	272	-138
	0.58	-58	334	-130
	0.86	-62	288	-119
	2.03	-52.7	281.7	-76.3
1.2	0	-29	290	-110
	0.33	-84	313	-82
	0.58	-56.33	290	-78.33
	0.86	-56	273	-83
	2.03	-52.3	291.7	-70

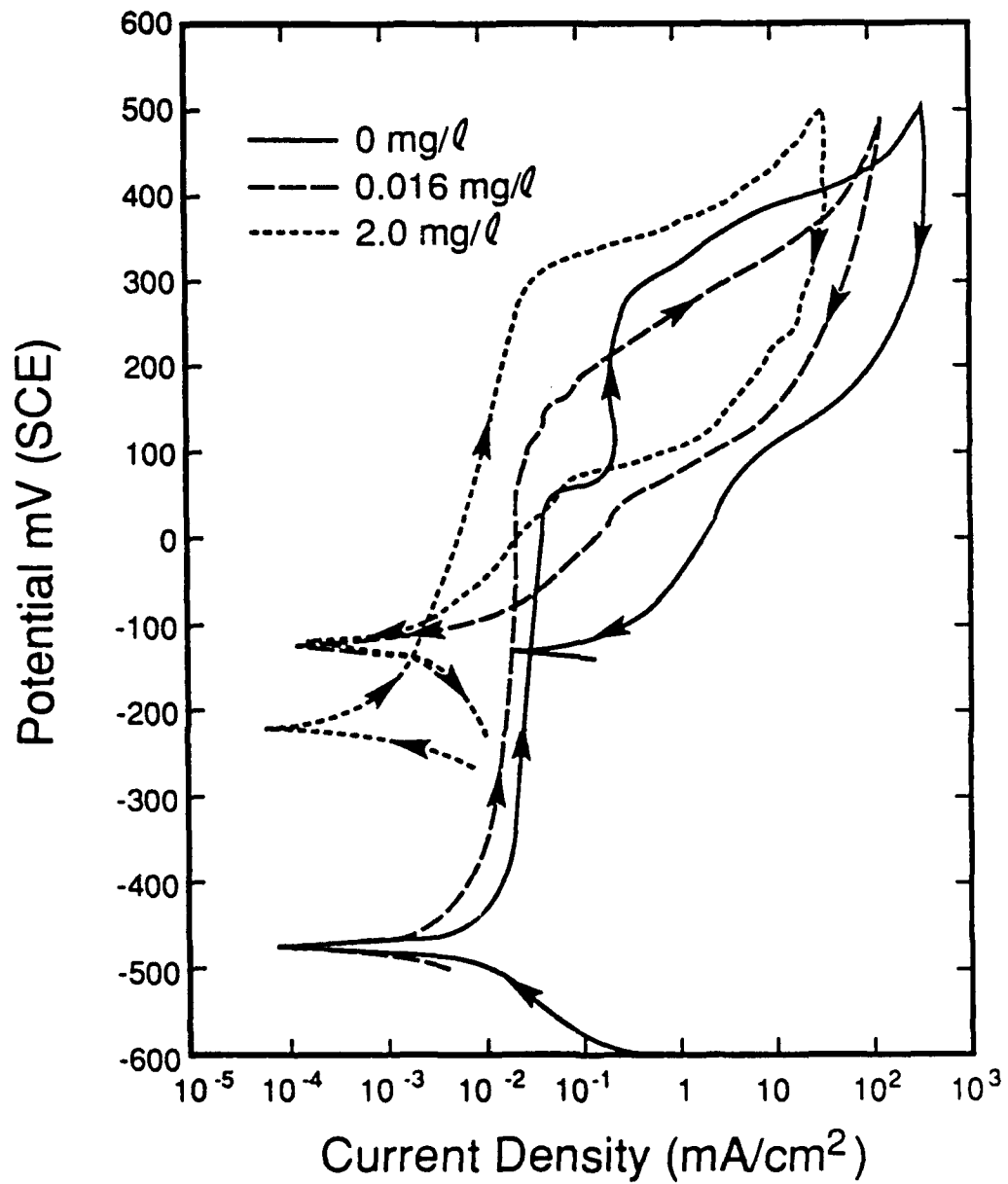


**Figure 3.** Cyclic polarization curves for 304L stainless steel as a function of ozone concentration in 0.5N NaCl.

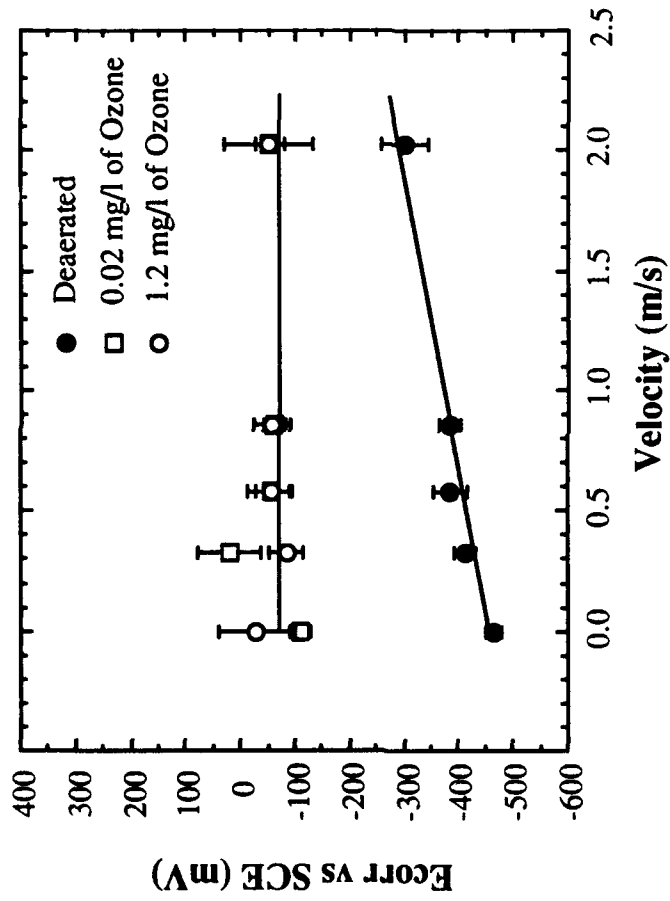


**Figure 4. Corrosion potential as a function of velocity in 0.5N NaCl solution at room temperature.**

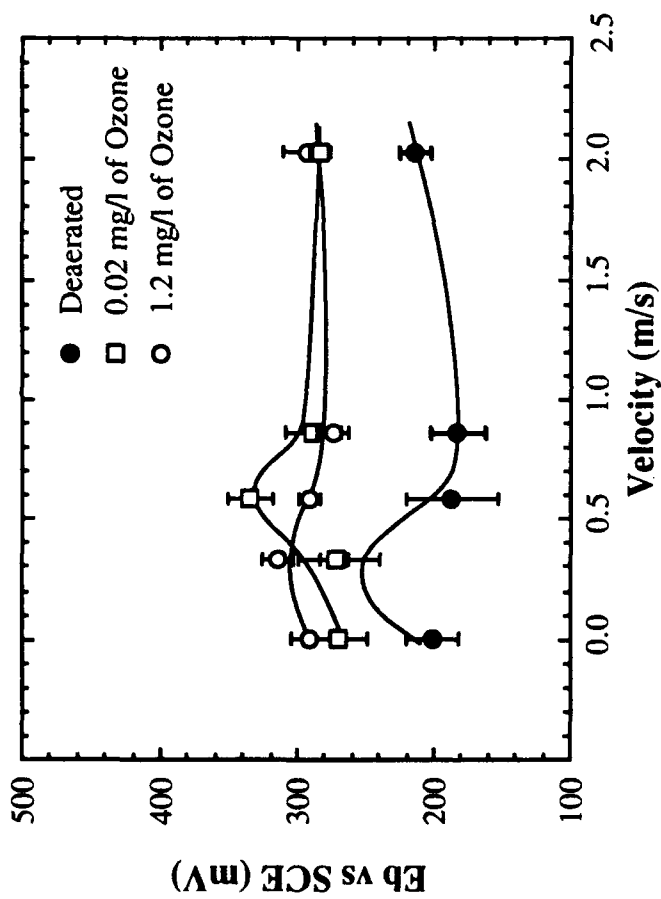


**Figure 5. Breakdown potential as a function of velocity in 0.5N NaCl solution at room temperature.**

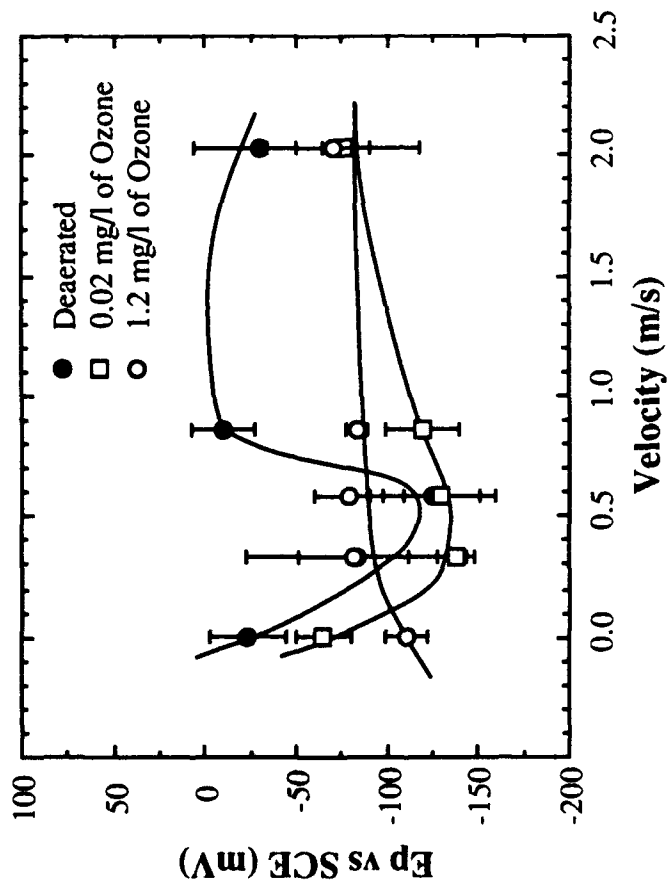


**Figure 6. Repassivation potential as a function of velocity in 0.5N NaCl solution at room temperature.**

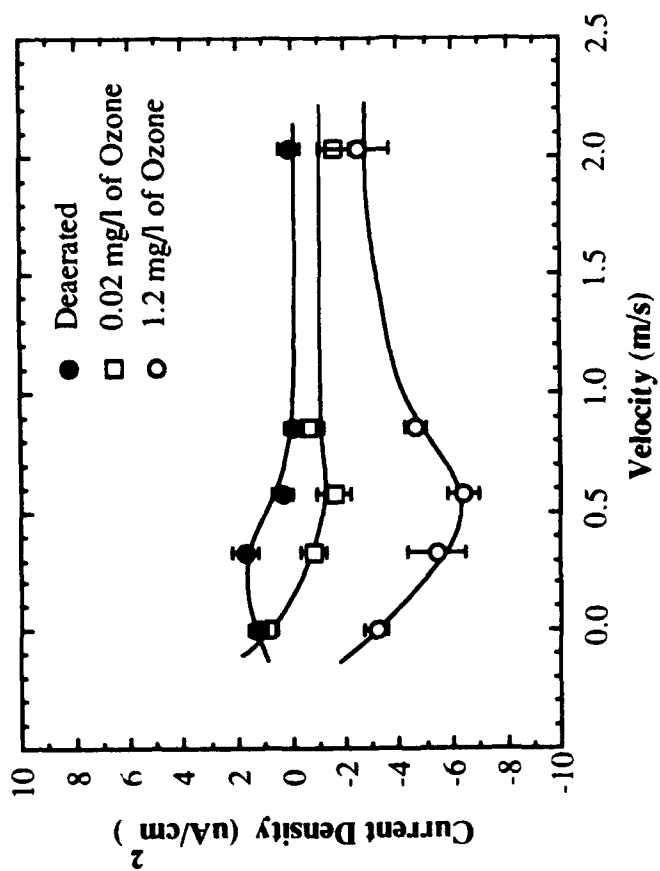


**Figure 7. Steady state current density measured after 10 minutes at a constant applied voltage of -100 mV vs. SCE.**